Linear correlation between binding energy and Young's modulus in graphene nanoribbons

Constantinos D. Zeinalipour-Yazdi[1,a)] and Constantinos Christofides[2]
[1]*Department of Chemistry, University of Cyprus, Nicosia 1678, Cyprus*
[2]*Department of Physics, University of Cyprus, Nicosia 1678, Cyprus*

(Received 18 May 2009; accepted 29 July 2009; published online 15 September 2009)

Graphene nanoribbons (GNRs) have been suggested as a promising material for its use as nanoelectromechanical reasonators for highly sensitive force, mass, and charge detection. Therefore the accurate determination of the size-dependent elastic properties of GNRs is desirable for the design of graphene-based nanoelectromechanical devices. In this study we determine the size-dependent Young's modulus and carbon-carbon binding energy in a homologous series of GNRs, $C_{4n^2+6n+2}H_{6n+4}$ $(n=2-12)$, with the use of all electron first principles computations. An unexpected linearity between the binding energy and Young's modulus is observed, making possible the prediction of the size-dependent Young's modulus of GNRs through a single point energy calculation of the GNR ground state. A quantitative-structure-property relationship is derived, which correlates Young's modulus to the total energy and the number of carbon atoms within the ribbon. In the limit of extended graphene sheets we determine the value of Young's modulus to be 1.09 TPa, in excellent agreement with experimental estimates derived for graphite and suspended graphene sheets. © *2009 American Institute of Physics*. [doi:10.1063/1.3211944]

I. INTRODUCTION

Graphene is an allotropic form of carbon found both in nature and artificially produced by chemical vapor deposition (CVD) of carbonaceous compounds.[1] Although stacks of this two-dimensional (2D) material have been known for more than a century[2] (i.e., graphite), recently there has been renewed interest in graphene in which some of the predictions of quantum electrodynamics such as the quantum Hall effect,[3–5] nonzero Berry's phase,[6] the Klein paradox,[7,8] chiral tunneling,[8] and massless Dirac fermions[9] are experimentally testable. Due to the unusual chemical and mechanical properties of nanographene (i.e., chemical inertness, robustness, and stiffness) graphene-based nanoelectromechanical systems (NEMSs) have also been proposed as the most sensitive material for fundamental engineering applications, such as mass, force, and charge detection using exfoliated graphene as an electromechanical resonator.[10–12] The elastic properties of nanosized elements may considerably differ from their extended analogs;[13] therefore, accurate knowledge of the size-dependent elastic properties of graphene nanoribbon (GNR) (i.e., Young, shear, and bend moduli, and Poisson's ratio) is desirable not only for the design of graphene-based NEMSs[12,14–16] but also for the future use of graphene in carbon-based electronic and magnetoelectronic devices[17–19] since the possibility of such deformations may considerably alter the electronic properties of GNRs.[20] Experimental determination of Young's modulus for graphene has only recently become possible through indentation experiments using atomic force microscopy (AFM).[14–16] Therefore, previous attempts have focused in calculating Young's modulus using various computational approaches, such as the membrane theory of shells,[21] molecular mechanics,[22] and various *ab initio* methods employing atom centered basis functions[23,24] and planewaves.[25]

The ideal structure of graphene consists of hexagonally arranged carbon atoms, each covalently bound to three neighboring carbons, through axial overlap of hybrid sp^2 orbitals. The remaining $2p_z$ orbitals on each carbon atom overlap in a parallel fashion resulting in a diffuse π-cloud located above and below the graphene layer. Stacks of graphene are held together by weaker dispersion interactions that result from polarization effects[26] of the diffuse π-clouds. The anisotropic intra- and interlayer interactions of the carbon atoms, evident by the drastically different nearest neighbor distance, known to be 1.42 and 3.35 Å, respectively, clearly assign nanographene as a 2D solid.[27–29]

The elastic properties are evaluated from first principles computations of relaxed and deformed GNRs of various sizes. The stress energy (ΔU_ε) of a GNR around equilibrium can be expanded in a Taylor series as a function of strain (ε) given by

$$\Delta U_\varepsilon = U(\varepsilon) - U(0) = \frac{\partial U(0)}{\partial \varepsilon}\varepsilon + \frac{1}{2}\frac{\partial^2 U(0)}{\partial \varepsilon^2}\varepsilon^2 + \frac{1}{6}\frac{\partial^3 U(0)}{\partial \varepsilon^3}\varepsilon^3 + \cdots, \quad (1)$$

where ε is defined as the fractional deformation in the direction of the applied strain given by

$$\varepsilon = \frac{\Delta l}{l}, \quad (2)$$

and $U(\varepsilon)$ and $U(0)$ are the total energies of the strained and fully relaxed ground-state structure of the GNR, respectively. By fitting the stress energy obtained from first principles computations with an nth order polynomial of the form $U(\varepsilon)=a\varepsilon+b\varepsilon^2+c\varepsilon^3+\cdots$ the coefficients a, b, c, etc., have

a)Electronic mail: zeinalip@ucy.ac.cy.

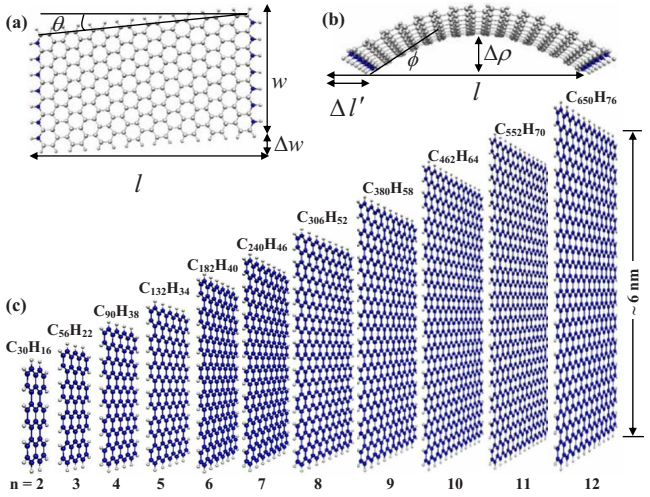

FIG. 1. (Color online) (a) Schematic of GNR ($C_{240}H_{46}$) under (a) shear and (b) bending stresses. (c) Homologous series of GNRs, $C_{4n^2+6n+2}H_{6n+4}$, examined for their elastic properties. Anchor atoms are indicated in black in (a) and (b).

been determined. In the limit of small deformations (strain/shear/bend $<5\%$) the linear and cubic coefficients were found to be negligible ($a,c \approx 0$), simplifying the strain, shear, and bending energy of the GNR to a simple quadratic form, which is given by

$$U(\varepsilon) \cong b\varepsilon^2, \tag{3}$$

$$U(\mu) \cong b'\mu^2, \tag{4}$$

and

$$U(\beta) \cong b''\beta^2, \tag{5}$$

respectively. From Eqs. (1) and (3) the in-plane Young's modulus is given by

$$E = \frac{2b}{V} = \frac{1}{V}\frac{\partial^2 U(0)}{\partial \varepsilon^2}, \tag{6}$$

where the GNR volume $V=wlh$, and the width (w) and the length (l) are the distances between edge carbon atoms at the middle of the armchair and zigzag edges (see Fig. 1) plus twice the van der Waals (vdW) radius of carbon in graphite[30] ($r_{vdW}=1.78$ Å). The height (h) was approximated from the interlayer separation of hexagonal graphite (3.354 Å).[28] The shear modulus (G) given from Eqs. (1) and (4) was evaluated using

$$G = \frac{2b'}{V} = \frac{1}{V}\frac{\partial^2 U(0)}{\partial \mu^2}, \tag{7}$$

where the shear stress is given as a function of the shear angle θ (where θ is small) defined in Fig. 1(a) and given by

$$\mu = \frac{\Delta w}{l} = \tan\,\theta. \tag{8}$$

The bending modulus (B) of the GNR is given by a similar relationship

$$B = \frac{2b''}{V} = \frac{1}{V}\frac{\partial^2 U(0)}{\partial \beta^2}, \tag{9}$$

where the bending stress (β) is given again by

$$\beta = \frac{\Delta l'}{l} = \frac{2\rho(\phi - \sin\,\phi)}{l}, \tag{10}$$

where ρ is the radius of curvature of the cylinder to which the GNR belongs to, and $\Delta l'$ is the in-plane deformation that causes the bending of the GNR by the angle ϕ defined in Fig. 1(b).

In this report we determine the elastic properties of GNRs and the size-dependent Young's modulus using all electron first principles computations. The elastic properties are determined in a systematic fashion for GNRs of varying size to the limiting case of an extended graphene sheet, and quantitative structure-property relationships (QSPRs) are derived that can be used to predict the size-dependent Young's modulus of GNRs on the basis of their total ground-state energy and the number of carbon atoms within the nanoribbon. It is noted that a linear correlation between the binding energy (BE) (sum of bond strengths) to Young's modulus has not been previously reported in literature to the best of the authors' knowledge.

II. COMPUTATIONAL METHODS

Relaxation of the atomic positions was obtained with the use of density functional theory (DFT) computations implemented in the NWCHEM (Refs. 31 and 32) code. The surface of graphene was modeled by a rectangular H-terminated GNR of varying size shown in Fig. 1 in order to saturate the dangling edge states. The models were either strained, sheared, or bent along the armchair, zigzag, or basal plane vectors, respectively, using carbon atoms of fixed nuclear positions (anchor atoms). In order to reduce the computational requirements, the GNR geometries, for straining and shearing deformations, were constrained within the D_{2h} and C_{2h} point group symmetries, whereas for bending deformations the structures were optimized within C_{2v} point group symmetry. The exchange and correlation effects were considered within the generalized gradient approximation using the commonly used Gaussian B3LYP hybrid exchange-correlation functional.[33,34] For the calculations standard molecular basis sets of the STO-3G*,[35,36] 6-31G*,[37] and aug-cc-pVDZ (Ref. 38) type have been adopted to test the convergence of basis set with respect to the elastic properties for the smallest GNR in the homologous series of molecules examined. The additional asterisk to the basis set denotes the inclusion of a shell of d polarization functions. The STO-3G* basis set was found to yield elastic properties to within 1% of the aug-cc-pVDZ basis for the larger molecular-weight GNR, therefore adopted for all subsequent calculations. Energetic minima for the smaller molecular-weight GNRs were confirmed by vibrational analysis, whereas the larger molecules were converged within the default convergence criteria. This resulted in maximum forces and the root-mean-square of the forces to be less than 0.01 and 0.001 eV/Å, respectively.

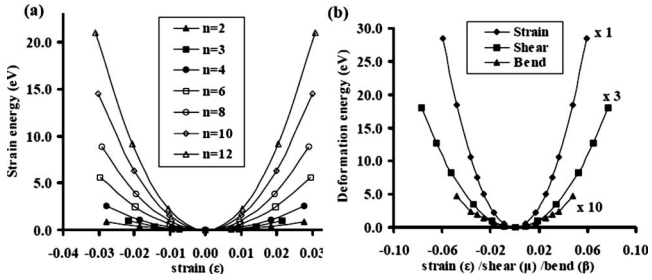

FIG. 2. (a) Strain energy as a function of strain for the various GNRs belonging to the homologous molecular sequence $C_{4n^2+6n+2}H_{6n+4}$, (b) Deformation energy as a function of strain, shear, and bending for $C_{240}H_{46}$ ($n=7$).

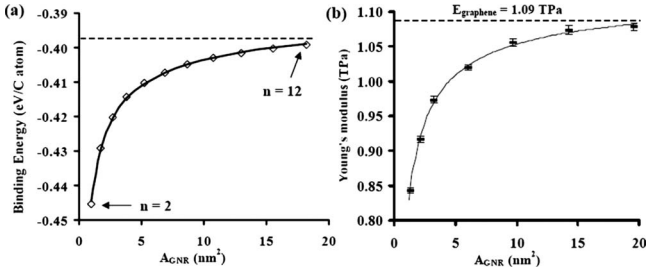

FIG. 3. (a) BE per carbon atom and (b) Young's modulus as a function of GNR surface area (A_{GNR}). The curved line is the nonlinear fit to the data using equations similar to the form of Eq. (13).

III. RESULTS AND DISCUSSION

Young's (E), shear (G), and bend (B) moduli were evaluated by compressing, shearing and bending the GNRs along the direction of the armchair and zigzag edges and the [0001] lattice vector, respectively, by translation of the anchor atoms. For the evaluation of the elastic properties all atomic positions, except the anchor atom, were fully relaxed. Typically the unstrained configurations were calculated first and then strain was applied in steps of 1% in units of strain percentage ($\varepsilon\%$) for strains less than 4%. The results of these simulations are presented in Fig. 2(a) and clearly demonstrate the parabolic form of the strain energy as a function of strain, reminiscent to the parabolic potential energy derived from Hook's law for macroscopic springs. It is interesting to note that the same strain can lead to increasingly high strain energies in the larger GNR, due to the additivity of the energy required to compress/elongate a larger number of carbon-carbon bonds, within the graphene network. In Fig. 2(b) we compare the deformation energies of the largest GNR examined for strain, shear, and bending deformations. On one hand, it is evident that any attempt to strain GNRs would result in bending of the basal plane of the GNR since for the same deformation the strain energy is one order of magnitude higher than the shear energy, in agreement with the rippling of suspended graphene sheets previously reported.[39] On the other hand, shear deformations do not drastically perturb the GNR internal energy, since they only involve bond angle changes, generally accompanied by smaller force constants. We note that for supported graphene, such as the case of graphite or supported graphene layers, the strain energy would have to overcome the dispersion forces between the layers of about 0.08 eV/C atom[26,40] (i.e., vdW interactions) for graphene layers to detach from their neighboring layers. Therefore for $C_{240}H_{46}$ the vdW interactions between two adjacent completely overlapping GNRs are about $U_{vdW}=19.2$ eV. From Eqs. (3) and (6) the relationship between strain and strain energy is given by

$$\varepsilon = \sqrt{\frac{2U(\varepsilon)}{EV}}. \tag{11}$$

So it is expected that bending of the supported GNR will occur when $U(\varepsilon) \geq U_{vdW}$, which in this particular case happens when the strain percentage exceeds the threshold value of 4.7%. This value should be useful for attempts to modify the electronic structure (i.e., bandgap opening) of GNR through mechanical deformations.[41]

For the evaluation of the elastic properties of extended GNRs (2D graphene) the BE per carbon atom was first converged with respect to the surface area of the GNR (see Fig. 3). The BE represents the stabilization of the carbon atoms within the GNR framework due to chemical bonding interactions, covalent in nature (i.e., σ and π bonds). The BE was obtained as the difference between the GNR total energy and that of the isolated carbon and hydrogen atoms calculated with the same basis set computed using

$$\mathrm{BE} = 2(E_{\mathrm{GNR}} - n_{\mathrm{C}}E_{\mathrm{C}} - n_{\mathrm{H}}E_{\mathrm{H}})/n_{\mathrm{C}}, \tag{12}$$

where E_{GNR}, E_C, and E_H are the total energies of the GNR, and the ground states of atomic carbon (triplet, −37.352 397 11Hr) and hydrogen (doublet, −0.467 532 59Hr), and n_C/n_H is the number of carbon/hydrogen atoms given by $4n^2+6n+2$ and $6n+4$ ($n=2-12$), respectively.

For the hydrogen terminated GNRs examined, we note that the size-dependent BE of the carbon network has the form

$$\mathrm{BE} = \mathrm{BE}_{\mathrm{bulk}} - \frac{C}{A_{\mathrm{GNR}}^{1/2}}, \tag{13}$$

where BE_{bulk} is the extrapolated BE of an extended graphene sheet, A_{GNR} is the basal plane area, and C is the size-dependent BE stabilization constant ($C=0.0543\pm0.0001$ eV nm/C atom) due to the gradual decrease in the edge effects as a function of the GNR surface area. The origin of these edge effects may be caused by various factors such as (a) edge states[42] as a result of quantum confinement, (b) edge stress[43,44] due to repulsive or attractive interactions between chemical moieties at the periphery of the GNR, and/or (c) Peierls[45] instability. In any case the edge effect causes considerable bond length alternation, especially at the armchair edge as we observe in our models, which increases the total energy of the GNR (E_{GNR}) due to bond compression and elongation at the periphery. Through Eq. (12) increase in E_{GNR} would cause considerable decrease in the BE (more exothermic), which as we demonstrate in Fig. 3(a) dissipates as a function of the lateral dimensions of the GNR. The same behavior is observed for Young's modulus and presumably for the remaining elastic properties (i.e., shear and bend moduli). It is evident that due to the delocalized electronic structure of GNRs there is a considerable expansion of the

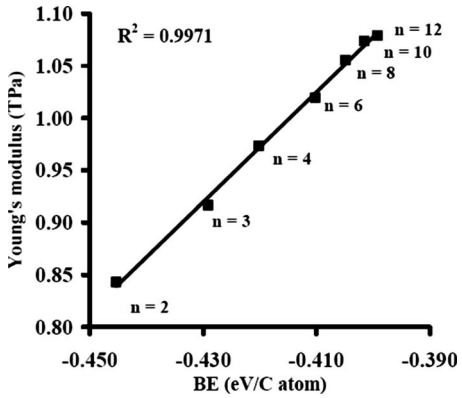

FIG. 4. Graph showing the linear correlation between the BE and Young's modulus of the homologous series of GNRs examined.

quantum confinement dimensions reaching widths as large as 6 nm in order to reach bulk properties. This is in contrast to other three-dimensional solids such as Si ⟨001⟩ nanowires[46] where the elastic properties converge at considerable smaller dimensions (~3–4 nm) due to their semiconducting properties, which are described by less diffuse electron densities at the Fermi level due to the existence of a bandgap. The findings here confirm that edge stress may be an important factor that regulates the size-dependent elastic properties in GNR.

In Fig. 4 we present an interesting linear correlation between E and BE in the homologous series of GNR examined, which in combination with Eq. (12) suggests that Young's modulus can be predicted on the basis of single point total energy calculations of the GNR ground state using the following relationship:

$$E = \frac{\omega}{(2n^2+3n+1)}[E_{\mathrm{GNR}} - (4n^2+6n+2)E_{\mathrm{C}} - (6n+4)E_{\mathrm{H}}] + \gamma, \quad (14)$$

where the coefficients ω and γ are given by 5.2622 (TPa C atom/eV) and 3.1824 (TPa), respectively. Note that these coefficients are accurate only when the B3LYP/STO-3G* method is used to evaluate the total energy, but in a similar manner these coefficients can be determined at any level of theory desirable. Such a nearly perfect linear correlation between the elastic properties and the BE energy is reported for the first time, although certain correlations of bond energies and forces' constants of isolated chemical bonds have previously been suggested.[47–49] An important advantage of this simple relationship is that such an assessment of E is computationally less tedious since it requires only a single point energy calculation. Furthermore one can extend the arguments here to the other elastic properties such as the shear and bend moduli.

It has been recently shown[50] that for GNR fragments, such as polycyclic aromatic hydrocarbons (PAHs), the total static molecular polarizability ($\bar{a}_{\mathrm{static}}$) is inversely proportional to the total molecular two-center exchange energy, a measure of the interatomic interactions, defined as

$$E_{\mathrm{exc}}(\mathrm{tot}) = \sum E_{\mathrm{exc}}(AB) = \sum\sum P_{\mu\lambda}P_{\nu\sigma}\langle\mu\lambda|\nu\sigma\rangle, \quad (15)$$

where $P_{\mu\lambda}$ and $P_{\nu\sigma}$ are the elements of the density matrix that describe the overlap between the atomic orbitals. Since this quantity is essentially $n_{\mathrm{C}}\mathrm{BE}/2$ in our treatment one can state that the static molecular polarizability of a GNR of arbitrary shape and dimensions (i.e., PAHs) is inversely proportional to the BE $\bar{a}_{\mathrm{static}} \propto 2/n_{\mathrm{C}}\mathrm{BE}$. This correlation combined with the so called "compressibility sum rule," from the many body theory of charged systems,[51] may provide a physical picture that explains the unexpected linearity we observe between E and BE since the polarizability (viewed as a response function to a charged field) is directly proportional to the compressibility, the inverse compressibility being equal to Young's modulus. We argue that when the GNR is uniaxially strained or stressed, the diffuse electron density at the Fermi level (mostly bound σ and π states), to which $\bar{a}_{\mathrm{static}}$ is mostly attributed to,[26,52] is polarized in the direction perpendicular to the basal plane of the GNR. This polarization decreases the effective polarizability $\bar{a}_{\mathrm{eff}}$ of the GNR in its deformed state. We note that once the deformation exceeds the proportional limit and $\bar{a}_{\mathrm{eff}}=0$, any further deformations reduce the interatomic interactions (BE) resulting in the converging trend commonly observed in stress-strain curves of 2D graphene.[25]

Using the extrapolated value of Young's modulus in the limit of extended graphene sheets in Fig. 3(b) we obtain an E of 1.09 TPa, in good agreement with periodic HF/6-31G* and planewave DFT calculations that determined 0.89–1.23 (Ref. 24) and 1.05 TPa,[25] respectively, and with the in-plane E of bulk graphite known to be 1 (Ref. 53) and 1.02 ± 0.03 TPa,[54] respectively; whereas a smaller agreement is observed in tip-induced deformation experiments using AFM for chemically derived single graphene sheets,[16] graphene stacks (less than 5),[14] and exfoliated graphene monolayers,[15] which have determined Young's moduli of 0.25, 0.5, and 1.0 TPa, respectively. Young's modulus in GNRs obtains the value of extended graphene sheets only when the lateral dimensions are larger than 8 nm (dimensions of $n=12$ GNR). It is therefore suggested that the suspended portion of the GNR used in graphene-based NEMS exceeds this threshold value; otherwise, Young's modulus and consequently the fundamental resonating frequency of the NEMS will be size dependent.

IV. CONCLUSIONS

We have determined Young's modulus (E) and carbon-carbon BE in a homologous series of GNRs, $\mathrm{C}_{4n^2+6n+2}\mathrm{H}_{6n+4}$ ($n=2-12$), with the use of all electron first principles computations. An interesting linearity between the BE and Young's modulus is observed, which is explained by the decrease in the molecular polarizability due to deformations within the proportional limit of GNRs. The unexpected linearity between E and BE makes possible the prediction of the size-dependent Young's modulus of GNRs through a single point energy calculation of the GNR ground state. A QSPR is derived that correlates Young's modulus to the total energy and the number of carbon atoms within the ribbon. In

the limit of extended graphene sheets we determine the value of Young's modulus to be 1.09 TPa in good agreement with experimental estimates derived for graphite and suspended graphene sheets.

ACKNOWLEDGMENTS

Fruitful discussions and comments on the manuscript from K. Moulopoulos are greatly acknowledged. We also thank A. Cooksy and C. Koutroulos for useful discussions. Computational work was performed under Environmental Molecular Sciences Laboratory (EMSL) Open Call Pilot Proposal No. 30392, a national user facility sponsored by the department's office for biological and environmental research located at the PNNL.

[1]T. A. Land, T. Michely, R. J. Behm, J. C. Hemminger, and G. Comsa, Surf. Sci. **264**, 261 (1992).
[2]H. Sjögren, Oef. Akad. Stockholm **41**, 29–53 (1884).
[3]V. P. Gusynin and S. G. Sharapov, Phys. Rev. Lett. **95**, 146801 (2005).
[4]N. M. R. Peres, F. Guinea, and A. H. Castro Neto, Ann. Phys. **321**, 1559 (2006).
[5]Y. Zheng and T. Ando, Phys. Rev. B **65**, 245420 (2002).
[6]G. P. Mikitik and Y. V. Sharlai, Phys. Rev. Lett. **82**, 2147 (1999).
[7]A. Calogeracos, Nat. Phys. **2**, 579 (2006).
[8]M. I. Katsnelson, K. S. Novoselov, and A. K. Geim, Nat. Phys. **2**, 620 (2006).
[9]S. Y. Zhou, G.-H. Gweon, J. Graf, A. V. Fedorov, C. D. Spataru, R. D. Diehl, Y. Kopelevich, D.-H. Lee, S. G. Louie, and A. Lanzara, Nat. Phys. **2**, 595 (2006).
[10]K. Ekinci, Y. Yang, and M. Roukes, J. Appl. Phys. **95**, 2682 (2004).
[11]B. Ilic, J. Appl. Phys. **95**, 3694 (2004).
[12]S. Bunch, A. M. van der Zande, S. S. Verbridge, I. W. Frank, D. M. Tanenbaum, J. M. Parpia, H. G. Craighead, and P. L. McEuen, Science **315**, 490 (2007).
[13]R. E. Miller and V. B. Shenoy, Nanotechnology **11**, 139 (2000).
[14]I. W. Frank, D. M. Tanenbauma, A. M. van der Zande, and P. L. McEuen, J. Vac. Sci. Technol. B **25**, 2558 (2007).
[15]C. Lee, X. Wei, J. W. Kysar, and J. Hone, Science **321**, 385 (2008).
[16]C. Gómez-Navarro, M. Burghard, and K. Kern, Nano Lett. **8**, 2045 (2008).
[17]Y. Zhang, Y.-W. Tan, H. L. Stormer, and P. Kim, Nature (London) **438**, 201 (2005).
[18]Y.-W. Son, M. L. Cohen, and S. G. Louie, Nature (London) **444**, 347 (2006).
[19]T. Enoki and Y. Kobayashi, J. Mater. Chem. **15**, 3999 (2005).
[20]L. Sun, Q. Li, H. Ren, H. Su, Q. W. Shi, and J. Yang, J. Chem. Phys. **129**, 074704 (2008).
[21]C. Pozrikidis, Int. J. Solids Struct. **45**, 732 (2008).
[22]A. Sakhaee-Pour, Solid State Commun. **149**, 91 (2009).
[23]K. N. Kudin, G. E. Scusceria, and B. Y. Yakobsen, Phys. Rev. B **64**, 235406 (2001).
[24]G. van Lier, C. van Alsenoy, V. van Doren, and P. Geerlings, Chem. Phys. Lett. **326**, 181 (2000).
[25]F. Liu, P. Ming, and J. Li, Phys. Rev. B **76**, 064120 (2007).
[26]C. D. Zeinalipour-Yazdi and D. P. Pullman, J. Phys. Chem. B **110**, 24260 (2006).
[27]Y. Baskin and L. Meyer, Phys. Rev. **100**, 544 (1955).
[28]J. D. Bernal, Proc. Phys. Soc., London, Sect. A **106**, 749 (1924).
[29]O. Hassel and H. Mark, Z. Phys. **18**, 291 (1924).
[30]A. Bondi, J. Phys. Chem. **68**, 441 (1964).
[31]E. J. Bylaska, W. A. de Jong, N. Govind, K. Kowalski, T. P. Straatsma, M. Valiev, D. Wang, E. Apra, T. L. Windus, J. Hammond, and P. Nichols, Pacific Northwest National Laboratory, Richland, WA, 2007.
[32]R. A. Kendall, E. Apra, D. E. Bernholdt, E. J. Bylaska, M. Dupuis, G. I. Fann, R. J. Harrison, J. Ju, J. A. Nichols, J. Nieplocha, T. P. Straatsma, T. L. Windus, and A. T. Wong, Comput. Phys. Commun. **128**, 260 (2000).
[33]A. D. Becke, J. Chem. Phys. **98**, 5648 (1993).
[34]C. T. Lee, W. T. Yang, and R. G. Parr, Phys. Rev. B **37**, 785 (1988).
[35]W. J. Hehre, R. F. Stewart, and J. A. Pople, J. Chem. Phys. **51**, 2657 (1969).
[36]W. Hehre, R. Ditchfield, R. Stewart, and J. Pople, J. Chem. Phys. **52**, 2769 (1970).
[37]R. Ditchfield, W. J. Hehre, and J. A. Pople, J. Chem. Phys. **54**, 724 (1971).
[38]D. E. Woon and T. H. Dunning, Jr., J. Chem. Phys. **98**, 1358 (1993).
[39]R. C. Thompson-Flagg, M. J. B. Moura, and M. Marder, Europhys. Lett. **85**, 46002 (2009).
[40]R. J. Good, L. A. Girifalco, and G. Kraus, J. Phys. Chem. **62**, 1418 (1958).
[41]G. Gui, J. Li, and J. Zhong, Phys. Rev. B **78**, 075435 (2008).
[42]K. Nakada, M. Fujita, G. Dresselhaus, and M. S. Dresselhaus, Phys. Rev. B **54**, 17954 (1996).
[43]S. Jun, Phys. Rev. B **78**, 073405 (2008).
[44]O. Hod, V. Barone, J. E. Peralta, and G. E. Scusceria, Nano Lett. **7**, 2295 (2007).
[45]R. E. Peierls, *Quantum Theory of Solids* (Clarendon, Oxford, 1955).
[46]B. Lee and R. E. Rudd, Phys. Rev. B **75**, 041305 (2007).
[47]R. G. Pearson, J. Mol. Struct. **300**, 519 (1993).
[48]M. Kaupp, B. Metz, and H. Stoll, Angew. Chem., Int. Ed. **39**, 4607 (2000).
[49]D. Cremer, A. Wu, A. Larsson, and E. Kraka, J. Mol. Model. **6**, 396 (2000).
[50]D. Martin, S. Sild, U. Maran, and M. Karelson, J. Phys. Chem. C **112**, 4785 (2008).
[51]D. Pines and P. Nozieres, *Theory of Quantum Liquids* (Benjamin, New York, 1966).
[52]C. D. Zeinalipour-Yazdi and D. P. Pullman, J. Phys. Chem. B **112**, 7377 (2008).
[53]B. Kelly, *Physics of Graphite* (Applied Science, Englewood, NJ, 1981).
[54]O. L. Blakslee, D. G. Proctor, E. J. Seldin, G. B. Spence, and T. Weng, J. Appl. Phys. **41**, 3373 (1970).